



Physiochemical and Antibacterial Studies of Two Tetradentate Ligands Type (N₂O₂) and Their Complexes with Co^{II}, Ni^{II} and Zn^{II} Ions

Hasan A. Hasan

Dept. of Chemistry/ College of Education for Pure Science (Ibn AL-Haitham)/
University of Baghdad

khaled salman

Dept. of Chemistry/ College of Education for Pure Science/ Al-Anbar
University

hasan_salehy@yahoo.com

Received in:22/June/2017, Accepted in:22/November/2017

Abstract

Two tetradentate ligands type (N₂O₂) and their complexes with Co^{II}, Ni^{II} and Zn^{II} ions were synthesized *via two steps*; in the first, the precursors W1 and W2 were synthesized from the reaction of 2,6-diamine pyridine or 2,4-diamine tolylene with 2,5-hexanedione respectively in a 2:1 mole ratio. In the second step the ligands [H₂L¹] and [H₂L²] were prepared from the reaction of the two precursor's with 2-hydroxy-1-naphthaldehyde in 1:2 mole ratio. Metal complexes were synthesized by the reaction of the ligands with equivalent amounts of the metal chloride. The prepared compounds were characterized with the physiochemical and spectral techniques which confirmed tetrahedral structure around the metal ions. The antibacterial activity of the ligands and complexes were screened.

Keywords: ligands type (N₂O₂), complexes and antibacterial activity.

Introduction

As a mixed donor systems, the Schiff bases may be considered the most important in the field of coordination chemistry. In the condensation reaction of the primary amines with an aldehyde or a ketone, C=O double bond replaced by a C=N double bond to form Schiff bases [1,2 & 3] In the transition metal complexes with Schiff base ligands, the coordination with metal ions through the azomethine nitrogen atom is studied due to selectivity, sensitivity and synthetic flexibility towards metal atoms [4]. Some Schiff bases can be derived from condensation of 2,6-diaminopyridine with other compounds, which are important in metal chelation, extraction, host-guest systems, antibiotics, enzyme mimics and natural products such as marine alkaloids[5,6]. Schiff bases containing 2-hydroxy-1-naphthaldehyde moiety coordinates to transition metal ions *via* deprotonation of phenolic hydroxyl at *o*-position and the imine nitrogen [7]. These kinds of Schiff base ligands possess high importance due to existence of (N-H \cdots O and O-H \cdots N) type hydrogen bonding tautomer between keto-enamine and enolimine forms [8]. The metal ion complexes have been used in medicine, toxicology and pharmacology. The high molecular weight polymers or Poly Schiff bases can be obtained by poly condensation of dialdehydes or diketones with aromatic or aliphatic diamine [9 & 10]. Some natural, non-natural, and natural-derived compounds have broad band of biological applications, this ability may correspond to the presence of azo-methine group in the structure of these compounds.

Experimental

Materials

The commercially available reagents were used without further purification.

Physical measurements

The precursors, ligands and their metal complexes were characterized using the following measurements: Elemental analyses (C, H, N) for ligands and their metal complexes were carried out on a Heraeus instrument (Vario EL) and Euro EA 3000. Melting points were obtained on a Buchi SMP-20 capillary melting point apparatus and are uncorrected. Infrared spectra were obtained as KBr discs using a Shimadzu 8300s FT-IR spectrophotometer in the range 4000-400 cm⁻¹. Electronic spectra were measured between 200-1100 nm with 10⁻³ M solutions in dimethylsulfoxide (DMSO) spectroscopic grade solvent at 25 °C using a Perkin-Elmer spectrophotometer Lambda. Thermogravimetric analysis was carried out using an STA PT-1000 Linseis company / Germany. NMR spectra (¹H, ¹³C- NMR) were acquired in DMSO-d⁶ solutions using a Bruker-300 and a JEOL-400MHz for ¹H-NMR and 75, 100.61 MHz for ¹³C-NMR, respectively with tetramethylsilane (TMS) as an internal reference. Metals were determined using a Shimadzu (A.A) 680 G atomic absorption spectrophotometer. Conductivity measurements were made with DMSO solutions using a Jenway 4071 digital conductivity meter at 25 °C. Magnetic moments at 303.8K were determined with a magnetic susceptibility balance (Sherwood Scientific).

Synthesis

Synthesis of precursors

Equivalent amount of 2,6-diaminepyridine or 2,4-diaminetolylene dissolved in ethanol (20ml) was added to a solution of 2,5-hexanedione (0.52g 4.58mmol) in ethanol (20ml) with stirring, also few drops of glacial acetic acid was added. The reaction mixture was refluxed for 4 hrs., then cooled and the precipitate was recrystallized in hot ethanol to yield [(1.20g, (88%), (1.00g,(77%))] from W₁ and W₂, respectively.

Synthesis of the ligands

To equivalent amount of the precursors (W₁) and (W₂) dissolved in 25 ml of methanol, it was added (1.16 g, 6.75mmol) of 2-hydroxy-1-naphthaldehyde in 10 ml of methanol with a few drops of glacial acetic acid as a catalyst, refluxed for 4 hrs., left at room temperature to 15 minutes, filtered off. The precipitate was collected with 10ml of cold dry methanol to yield [1.4g, 70%, m.p=(228-230) °C and 1.3g, 67%, m.p. = (178-180)°C] of [H₂L¹] and [H₂L²], respectively.

Synthesis of the complexes

Synthesis of [CoL¹] complex

To a solution of (0.40 g, 0.660mmole) of the ligand [H₂L¹] dissolved in (40ml) of ethanol, it was added (0.074g, 1.322mmol) of potassium hydroxide dissolved in 10 ml ethanol with stirring and heating. Then (0.157) g, 0.661mmol) of Cobalt (II) chloride hexahydrate dissolved in 10 ml ethanol was added to ligand solution.

The resulting mixture was refluxed for 2 hrs. filtered off then washed with absolute ethanol and recrystallized from ethanol. (Yield: 0.33g, %75) m.p.= (272-275) °C.

Synthesis of [H₂L¹] and [H₂L²] complexes

A similar method to that mentioned in the preparation of Co^{II} complex was used to prepare the other complexes, the quantity of the other reagents was adjusted accordingly; table (1) shows the physical properties of the complexes and their reactant quantity.

Table (1): Some physical properties of the prepared [H₂L¹], [H₂L²] complexes and their reactant quantity

Empirical formula	Color	m.p. °C	Wt of metal salt (g)	Wt of product (g)	Yield %
[CoL ¹]	Brown	(272-275)	0.157	0.33	75
[ZnL ¹]	Dark brown	Dec over(320)	0,157	0.37	84
[NiL ¹]	Light yellow	Dec over(320)	0.112	0.35	81
[CoL ²]	Light brown	Dec over(320)	1.508	0.34	79
[ZnL ²]	Pal brown	Dec over(320)	0.863	0.34	77
[NiL ²]	Olivy	Dec over(320)	1.507	0.29	66

Dec. = Decomposed

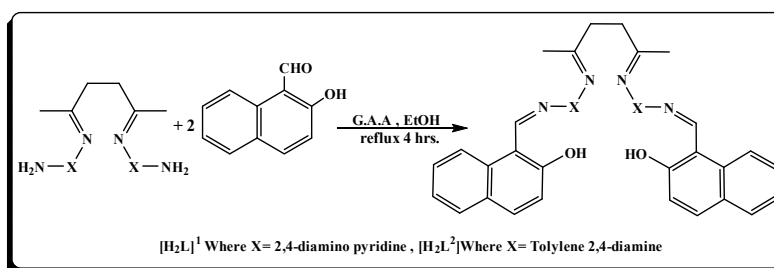
Results and discussion

The precursors W_1 and W_2 were synthesized by the reaction of 2,5-hexanedione with 2,6-diaminopyridin and with 2,4-diaminotolylene, respectively, in 1:2 mole ratio using ethanol as a solvent according to the general synthetic route shown in scheme (1). The precursors were characterized by FT-IR spectroscopy and melting point measurements.

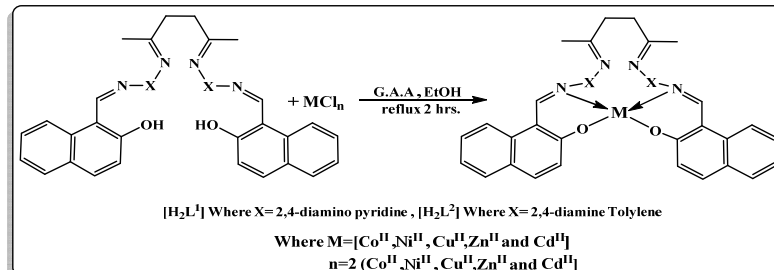
The potentially two tetradenate ligands type N_2O_2 donor atoms have been synthesized. The ligands contain two labile protons $[H_2L^1]$ and $[H_2L^2]$, by removing these protons an anionic (-2) tetradentate system is formed.

The ligands $[H_2L^1]$ and $[H_2L^2]$ were synthesized by the condensation reaction of precursors $[W_1]$ and $[W_2]$ with 2-hydroxy-1-naphthaldehyde, respectively in, 1:2 mole ratio using methanol as a solvent according to the general route shown in Scheme (1).

The method used to prepare all complexes involves the reaction of the ligands with metal chloride in 1:1 mole ratio at reflux in ethanol and pure complexes were formed, Scheme (2).



Scheme (1): Synthesis route of the ligands



Scheme (2): Synthesis route of complexes

I.R Spectra

FT-IR spectral data for $[H_2L^1]$ and $[H_2L^2]$

Spectra of the precursors shows bands at $[(3391), (3377) \text{ cm}^{-1}]$ and $[(3381), (3354) \text{ cm}^{-1}]$ could be attributed to asymmetrical and symmetrical stretching of primary amine $\nu(\text{NH}_2)$ in W_1 and W_2 , respectively. The $\nu(\text{C}=\text{O})$ stretching at 1710 cm^{-1} in the hexandion spectrum disappeared in the precursors spectra indicating the formation of the Schiff base precursors [11,12,13].

The ligands spectra, figures (1) and (2) show the disappearing of carbaldehydic $\nu(\text{C}=\text{O})$ stretching at $(1650) \text{ cm}^{-1}$ and the amine stretching of the precursors moiety $[(3391), (3377) \text{ cm}^{-1}]$ and $[(3381), (3354) \text{ cm}^{-1}]$. Also the spectra show appearing of two azomethen bands at $(1626) \text{ cm}^{-1}$ and $(1630) \text{ cm}^{-1}$ of $[H_2L^1]$ and $[H_2L^2]$, respectively. The disappearing of the carbonyl and amine groups and appearing of the imine groups revealing the formation of the ligands. Finally, the spectra show bands at $(3440) \text{ cm}^{-1}$ and $(3400) \text{ cm}^{-1}$ for $[H_2L^1]$ and $[H_2L^2]$,

respectively, assignable for interference of the two OH phenolic groups in each ligand [14,15,16]. The spectrum of $[H_2L^1]$ shows a band at $(1532) \text{ cm}^{-1}$ may be attributed to $\nu(C=N)_{\text{imino}}$ of pyridine moiety, while the band at 2926 cm^{-1} in the $[H_2L^2]$ spectrum may be assigned to the ring methyl group.

The infrared spectra of the complexes exhibited broad bands at the range $(3215-3381) \text{ cm}^{-1}$ for complexes, that may be attributed to the OH group of the adsorbed water molecules [18]. The detected bands at $(1626) \text{ cm}^{-1}$ and $(1630) \text{ cm}^{-1}$ which assigned to the stretching vibration of the azomethine group $\nu(C=N)$ of the free ligands $[H_2L^1]$ and $[H_2L^2]$, respectively, this band is shifted to the range $(1587-1630) \text{ cm}^{-1}$ in the complexes, the shift to lower frequency may be due to delocalization of metal electron density into the ligand π -system [18] (HOMO \rightarrow LUMO).

In the spectra of the metal complexes the $\nu(C-O)$ band underwent a shift towards lower and higher frequencies and appeared at the range $(1200-1255) \text{ cm}^{-1}$ in the complexes, and this shift confirms the participation of oxygen in the (C-O-M) bond. On the other hand, in the infrared spectra of the complexes, new absorption bands at the range $[(505)-(577) \text{ and } (417)-(459)] \text{ cm}^{-1}$, were observed indicating the $\nu(M-O)$ and $\nu(M-N)$ bonds, in the complexes [19]. The assignment of characteristic bands is summarized in table (2).

Table (2): Infrared spectral data (wave number ν) cm^{-1} of the ligands $[H_2L^1]$, $[H_2L^2]$ and their metal complexes

Compound	$\nu(\text{O-H})$	$\nu(\text{C-H})$	$\nu(\text{C=N})_{\text{imino}}$	$\nu(\text{C=C})_{\text{arom.}}$	$\nu(\text{C-O})$	$\nu(\text{M-O})$	$\nu(\text{M-N})$
$[H_2L^1]$	3400 (br)	-	1626 (s)	1610	-	-	-
$[\text{CoL}^1]$	-	2920	1630 (s)	1539	1200 (w)	511 (w)	459 (w)
$[\text{ZnL}^1]$	3334	2931 (m)	1593 (s)	1450	1246 (w)	577 (w)	451 (w)
$[\text{NiL}^1]$	3350	2925	1614	1545	1250	505	420
$[H_2L^2]$	3400 (br)	-	1630 (s)	1574	-	-	-
$[\text{CoL}^2]$	3365	2924 (m)	1610 (s)	1531	1254 (w)	573 (w)	459 (w)
$[\text{ZnL}^2]$	3215	2924 (m)	1606 (s)	1539	1255 (w)	561 (w)	451 (w)
$[\text{NiL}^2]$	3381	2924	1610	1535	1255	573	478

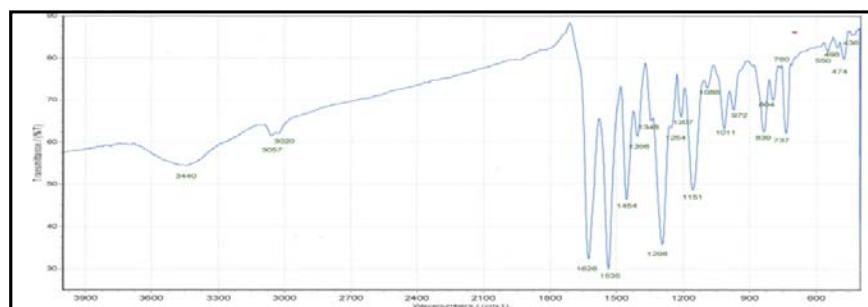
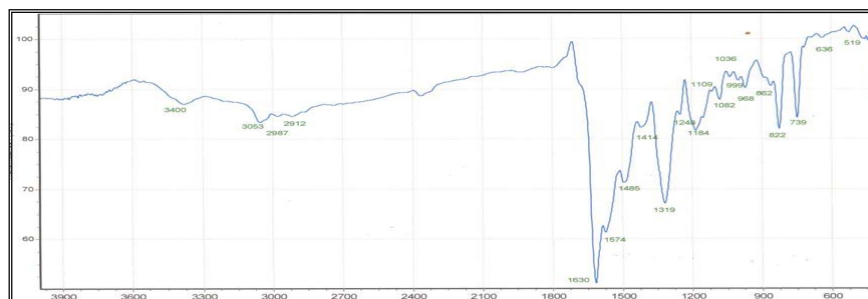
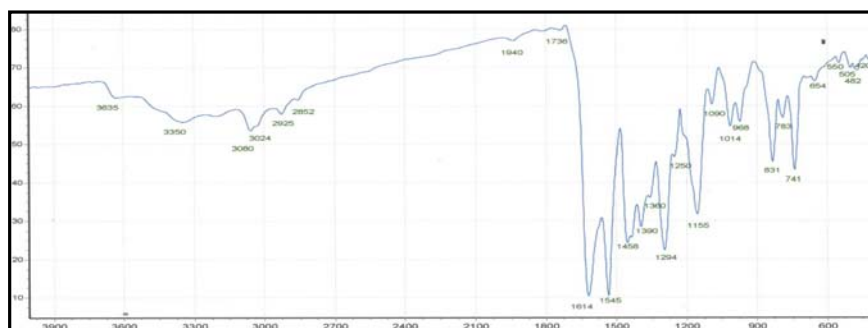
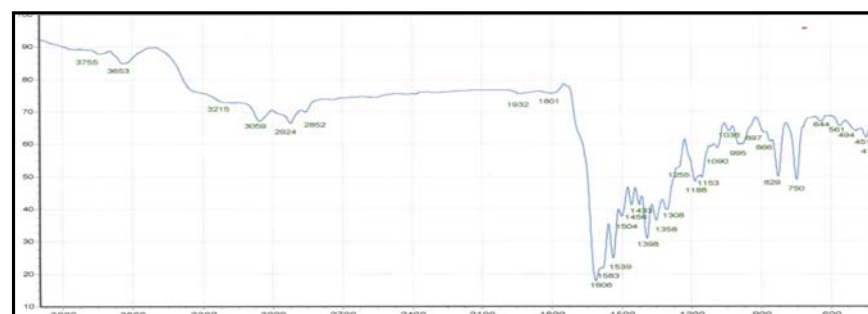


Figure (1): FT-IR spectrum of the ligand $[H_2L^1]$

Figure (2): FT-IR spectrum of ligand $[H_2L^2]$ Figure (3): FT-IR spectrum of $[NiL^1]$ complexFigure (4): FT-IR spectrum of $[ZnL^2]$ complex

Electronic spectra

Peaks of shortness wave length figures (5) and (6) at [(265 nm) (37735 cm^{-1}) ($\epsilon_{\text{max}}=10171\text{ molar}^{-1}\text{cm}^{-1}$) and (311nm) (32154 cm^{-1}) ($\epsilon_{\text{max}}=1076\text{ molar}^{-1}\text{ cm}^{-1}$)] and [(276 nm) (36231cm^{-1}) ($\epsilon_{\text{max}}=2291\text{ molar}^{-1}\text{cm}^{-1}$) (301 nm) (3322 cm^{-1}) ($\epsilon_{\text{max}}=2291\text{ molar}^{-1}\text{ cm}^{-1}$)] may be due to $\pi\rightarrow\pi^*$ transition of the aromatic rings of Schiff's base ligands $[H_2L^1]$ and $[H_2L^2]$, respectively [20]. The peaks at the ranges (380-475) and (361-460) may be assigned to interference of the ($n\rightarrow\pi^*$) transitions of azomethane groups and hydroxyl moiety in ligands $[H_2L^1]$ and $[H_2L^2]$, respectively [21,22]. The absorption data of the prepared ligands are given in table (3). The absorption peaks of the complexes were summarized in table (4). In the complexes spectra, it was shown intense peaks in the (U.V) region at the range [(270nm) (37037 cm^{-1}) ($\epsilon_{\text{max}}=1890\text{ molar}^{-1}\text{ cm}^{-1}$) and (301 nm) (33222 cm^{-1}) ($\epsilon_{\text{max}}=2112\text{ molar}^{-1}\text{ cm}^{-1}$)] and [(267) nm) (37453 cm^{-1}) ($\epsilon_{\text{max}}=1432\text{ molar}^{-1}\text{ cm}^{-1}$) and (313 nm) (31948 cm^{-1}) ($\epsilon_{\text{max}}=1181\text{ molar}^{-1}\text{ cm}^{-1}$)] can be assigned to ($\pi\rightarrow\pi^*$) transitions. The ($n\rightarrow\pi^*$) peaks at the ranges (380-475nm) and (361-460) in free ligands shifted to longer wave lengths in the complexes as a result of coordination to the metal

ion and appeared as broad bands (due to interference with charge transfer transitions) at the range (347-520nm). Finally, the peaks in the visible region can be assigned with d-d transitions. The Co^{II} complexes, figures (7) and (8) show peaks at (746 nm) and (696) may be assignable to ${}^4\text{A}_2(\text{F}) \rightarrow {}^4\text{T}_2(\text{F})$ transition of $[\text{CoL}^1]$ and $[\text{CoL}^2]$, respectively, suggesting tetrahedral geometry around Co^{II} ion. The results were in a good agreement with results reported [23 & 24]. The Ni^{II} complexes show peaks at (744 nm) and (756nm) assignable to ${}^3\text{T}_1 \rightarrow {}^3\text{T}_1(\text{F})$ transition of $[\text{NiL}^1]$ and $[\text{NiL}^2]$ suggesting tetrahedral geometry around Ni^{II} ion. The results were in a good agreement with results reported [24]. The Zn^{II} metal ion of complexes belongs to d^{10} system and these metals do not show (d-d) transition. Tetrahedral geometry was proposed around Zn^{II} ions. The results were in a good agreement with results reported [23].

Table (3): Electronic spectral data of ligands $[\text{H}_2\text{L}^1]$ and $[\text{H}_2\text{L}^2]$

Compound	λ (nm)	$\nu^- \text{cm}^{-1}$	$\epsilon_{\text{molar}} \text{cm}^{-1}$	Assignments
$[\text{H}_2\text{L}^1]$	265	37735	1017	$\pi \rightarrow \pi^*$
	311	32154	1076	
	(380-475)			$n \rightarrow \pi^*$
$[\text{H}_2\text{L}^2]$	276	36231	2332	$\pi \rightarrow \pi^*$
	301	3322	2291	
	(361-460)			$n \rightarrow \pi^*$

Table (4): Electronic spectral data of $[\text{H}_2\text{L}^1]$, $[\text{H}_2\text{L}^2]$ and its metal complexes

	Nm	cm^{-1}			
$[\text{CoL}^1]$	270	37037	1890	$\pi \rightarrow \pi^*$	Tetrahedral
	301	33222	2112		
	(376-515)			$n \rightarrow \pi^* + \text{Charge transfer}$	
$[\text{NiL}^1]$	746	13404	47	${}^4\text{A}_2(\text{F}) \rightarrow {}^4\text{T}_2(\text{F})$	Tetrahedral
	271	36900	2023	$\pi \rightarrow \pi^*$	
	314	31847	1724		
	(370-516)			$n \rightarrow \pi^* + \text{Charge transfer}$	
$[\text{ZnL}^1]$	744	13440	38	${}^3\text{T}_1 \rightarrow {}^3\text{T}_1(\text{F})$	Tetrahedral
	267	37453	1432	$\pi \rightarrow \pi^*$	
	313	31948	1181		
$[\text{CoL}^2]$	(378-505)			$n \rightarrow \pi^* + \text{Charge transfer}$	Tetrahedral
	271	36900	1952	$\pi \rightarrow \pi^*$	
	314	31847	1992		
$[\text{NiL}^2]$	(350-502)			$n \rightarrow \pi^* + \text{Charge transfer}$	Tetrahedral
	696	14367	14	${}^4\text{A}_2(\text{F}) \rightarrow {}^4\text{T}_2(\text{F})$	
	272	36764	1890	$\pi \rightarrow \pi^*$	
	298	33557	1270		
$[\text{ZnL}^2]$	(380-490)			$n \rightarrow \pi^* + \text{Charge transfer}$	Tetrahedral
	756	13227	22	${}^3\text{T}_1 \rightarrow {}^3\text{T}_1(\text{F})$	
	275	36363	2202	$\pi \rightarrow \pi^*$	
305	24752	2210			
$[\text{ZnL}^2]$	(347-475)			$n \rightarrow \pi^* + \text{Charge transfer}$	Tetrahedral

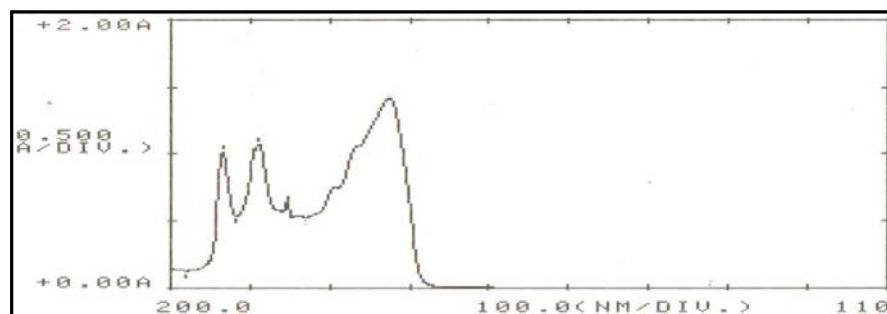


Figure (5): Electronic spectrum of the ligand [H₂L¹]

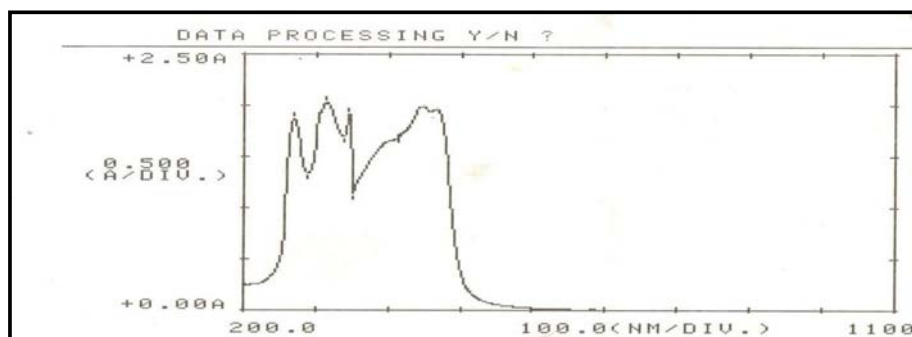


Figure (6): Electronic spectrum of the ligand [H₂L²]

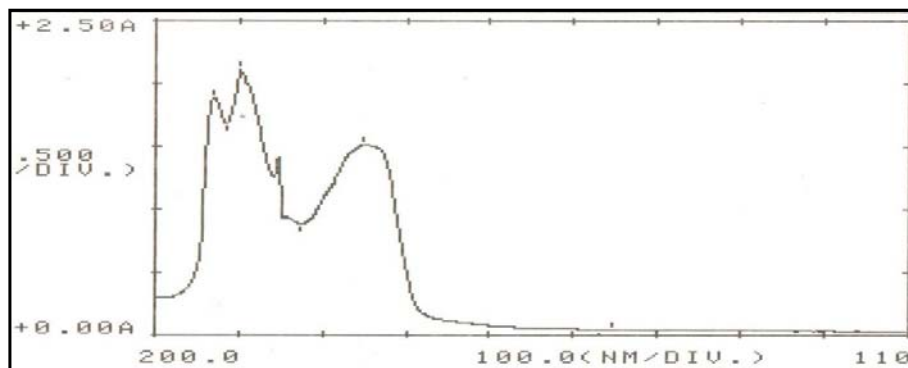


Figure (7): Electronic spectrum of [CoL¹] Complex

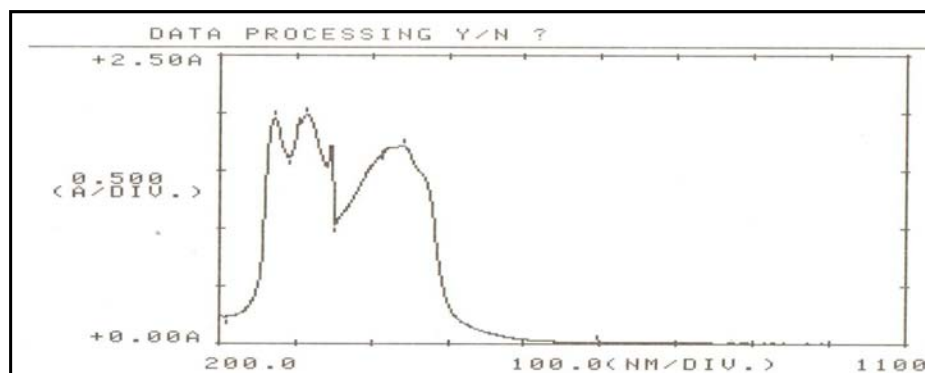


Figure (8): Electronic spectrum of $[\text{CoL}^2]$ complex

NMR spectra

The ^1H -NMR and ^{13}C -NMR analysis were used to characterize the $[\text{H}_2\text{L}^1]$, $[\text{H}_2\text{L}^2]$, $[\text{ZnL}^1]$ and $[\text{ZnL}^2]$. The spectra were recorded in DMSO-d_6 solution. Figure (9), shows the ^1H -NMR spectrum of the prepared Schiff base ligand $[\text{H}_2\text{L}^1]$ in DMSO-d_6 . A single chemical shift of the OH proton in the carbaldehyde ring observed at ($\delta=15.19$ ppm, 1H) due to intramolecular hydrogen bonding with the nitrogen atom of the imine group [25]. The spectrum showed chemical shift at ($\delta=1.19$ ppm, m, 6 H) can be assigned to the methyl (CH_3) group protons, while the chemical shift at ($\delta=0.86$ ppm, 4H) may be attributed to the methylene (CH_2) group protons. Multiplet chemical shifts around ($\delta=6.93$ - 8.19 ppm, m, 18 H) may be assigned to protons of aromatic rings [26]. Finally, the spectrum showed a chemical shift may be assigned to the iminic ($-\text{CH}=\text{N}$) proton at ($\delta=10.02$ ppm, s, 1H) of the free ligand [26]. The results are summarized in table (5).

^1H -NMR spectrum of the $[\text{ZnL}^1]$ complex shown in figure (10), includes the same functional groups with a shift in the positions. The OH resonance disappeared in the spectrum as expected, revealing coordination with metal ion after deprotonation. The results are summarized (6). ^1H -NMR spectrum of Schiff base ligand $[\text{H}_2\text{L}^2]$ in DMSO-d_6 shown in Fig. (11). Single atchemical shift of the OH proton at 5.7 ppm as exprotonation, because it was established that the investigated Schiff bases exist as NH tautomers in DMSO-d_6 solution with NH group orientated in *cis* position relative to the carbonyl of naphthylidene moiety [27]. The same interpretations mentioned for $[\text{H}_2\text{L}^1]$ can be used in explanation of $[\text{H}_2\text{L}^2]$ ^1H -NMR spectrum. The results are summarized in table (7).

^1H -NMR spectrum of the $[\text{ZnL}^2]$ complex was shown in figure (12), the same interpretations mentioned for $[\text{ZnL}^1]$ can be used in explanation of $[\text{ZnL}^2]$ spectra. The results are summarized in table (8).

The ^{13}C -NMR spectrum of $[\text{H}_2\text{L}^2]$, figure (13) in DMSO-d_6 solvent shows a chemical shift at the range ($\delta=108.46$ - 129.02) ppm can be attributed to (C-C), (C-N) and (C-O) groups. The chemical shifts at the range ($\delta=131.72$ - 143.21) ppm can be attributed to aromatic (C=C). The chemical shifts at (155.28-155.57) ppm may refer to azomethene (C=N) groups [26]. Finally, the chemical shift at ($\delta=171.71$) ppm can be attributed to (C=O) group resulted from tautomerism [15]. The results are summarized in table (9).

Same chemical shifts were appeared in the ^{13}C -NMR spectrum of $[\text{ZnL}^2]$, figure (14) in DMSO-d_6 solvent, but the chemical shift of azomethene (C=N) groups shows a shifting at low field and appeared at (161.68) ppm may be due to coordination to the metal ion. The results are summarized in table (10).

Table (5): $^1\text{H-NMR}$ spectral data for $[\text{H}_2\text{L}^1]$ measured in DMSO-d^6 and chemical shift in ppm (δ)

Compound	Funct. Group	δ (ppm)
$[\text{H}_2\text{L}^1]$	O-H	(15.19) (1H, S)
	(-CH=N)	(10.02) (1H,S)
	CH_3	(1.19) (6H)
	Ar-H	(6.93-8.19) (18Hm)
	CH_2	(0.86) (4H)

Table (6): $^1\text{H-NMR}$ spectral data for $[\text{ZnL}^1]$ measured in DMSO-d^6 and chemical shift in ppm (δ)

Compound	Funct. Group	δ (ppm)
$[\text{ZnL}^1]$	Ar-H	($\delta=6.67-8.00$) (18 H,m)
	(-CH=N)	($\delta=9.54$) (1H,S)
	CH_3	($\delta=1.2-1.4$) (6H,S)
	CH_2	($\delta=0.7-0.9$) (4H)

S= single, m = multiple

Table (7): $^1\text{H-NMR}$ spectral data for $[\text{H}_2\text{L}^2]$ measured in DMSO-d^6 and chemical shift in ppm (δ)

Compound	Funct. Group	δ (ppm)
$[\text{H}_2\text{L}^2]$	OH	(5.8) (1H, S)
	CH_3	(1.22)(6H,s)
	CH_3 (tolyle)	(2.17)(6H,s)
	Ar-H	(7.02-8.56) (18H,m)
	CH_2	(0.83) (4H,s)
	(-CH=N)	(9.80-9.95) (1H,S)

S= singlet, m= multiple

Table (8): $^{13}\text{C-NMR}$ spectral data for $[\text{ZnL}^2]$ measured in DMSO-d^6 and chemical shift in ppm (δ)

Compound	Funct. Group	δ (ppm)
$[\text{ZnL}^2]$	C-C,C-N	108.61-129.88
	C-O	130.15-137.77
	C=C aromatic	141.72
	C=N	161.68

S= singlet, m= multiple

Table (9): Microanalysis and physical properties for the ligands [H₂L¹], [H₂L²] and its complexes

Compound	Λ_m S.cm ² molar ⁻¹	μ_{eff} B.M. expt.	Found (calc.) %		
			C	H	N
[H ₂ L ¹]	-	-	(75.48)	(5.33)	(13.90)
			75.20	5.53	13.24
[H ₂ L ²]	-	-	(79.97)	(6.07)	(8.88)
			79.96	5.87	8.05
[CoL ¹]	16.60	4.411			
[NiL ¹]	13.40	3.800			
[ZnL ¹]	5.90	-			
[CoL ²]	9.43	4.497			
[NiL ²]	2.96	4.000			
[ZnL ²]	20.00	-			

(calc.) = calculate

Table (10): Bacterial activity [H₂L¹], [H₂L²] and its complexes

NO.	Compounds	Escherichia coli(G ⁻)	Enterobacter cloacae(G ⁻)	Bacillus stuttilis(G ⁺)	Staphylococcus aureus(G ⁺)
1	Control	-	-	-	-
2	H ₂ L ₁]	-	10	10	10
3	[CoL ₁]	-	-	11	-
4	[NiL ₁]	-	-	12	-
5	[ZnL ₁]	-	-	18	12
6	H ₂ L ₂]	-	12	10	-
7	[CoL ₂]	-	-	13	12
8	[NiL ₂]	-	-	-	-
9	[ZnL ₂]	-	20	19	-

(-) =No activity

Figure (8): Electronic spectrum of [CoL²] complex

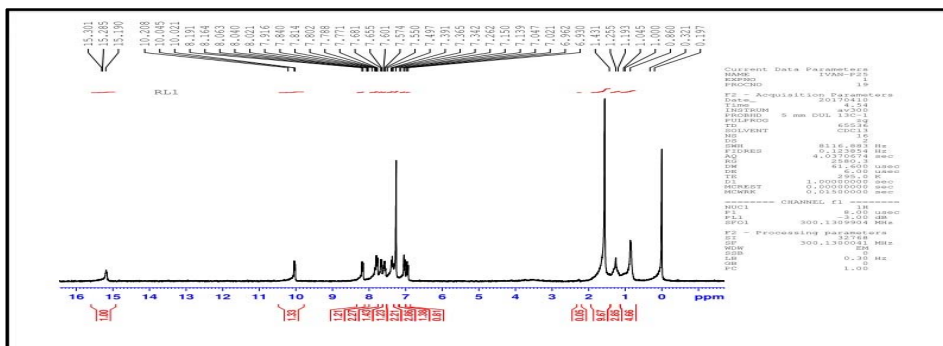


Figure (9): ¹H-NMR spectrum of the ligand [H₂L¹]

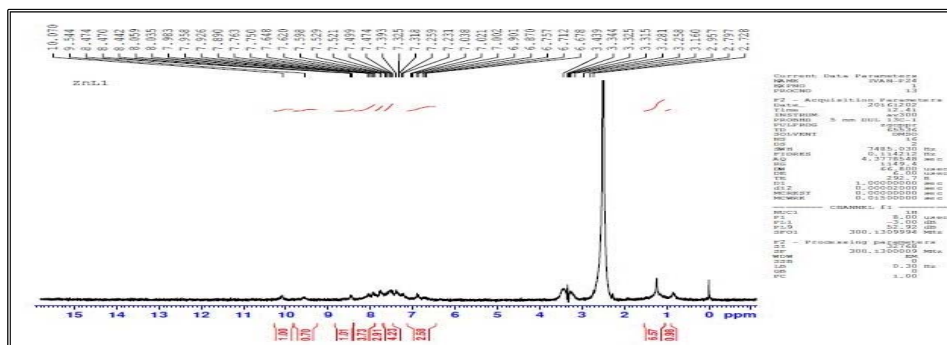


Figure (10): ¹H-NMR spectrum of [ZnL¹] complex

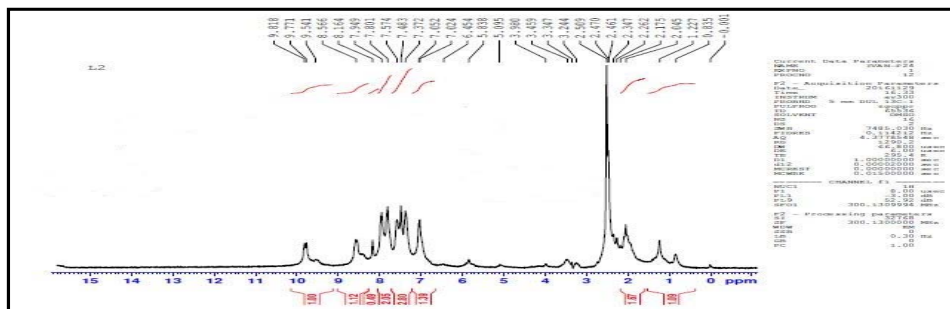


Figure (11): ¹H-NMR spectrum of the ligand [H₂L²]

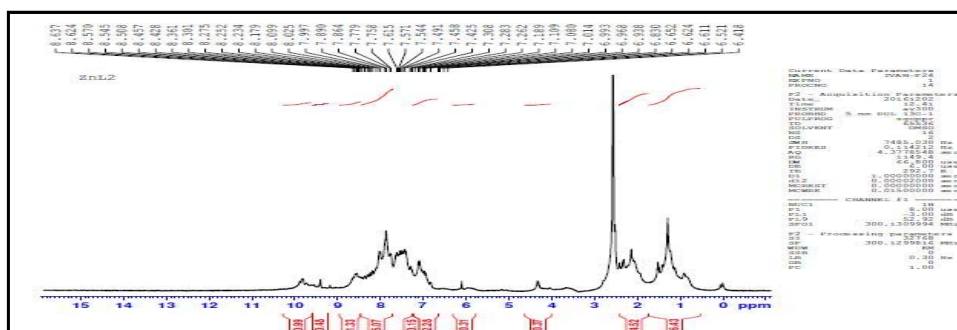
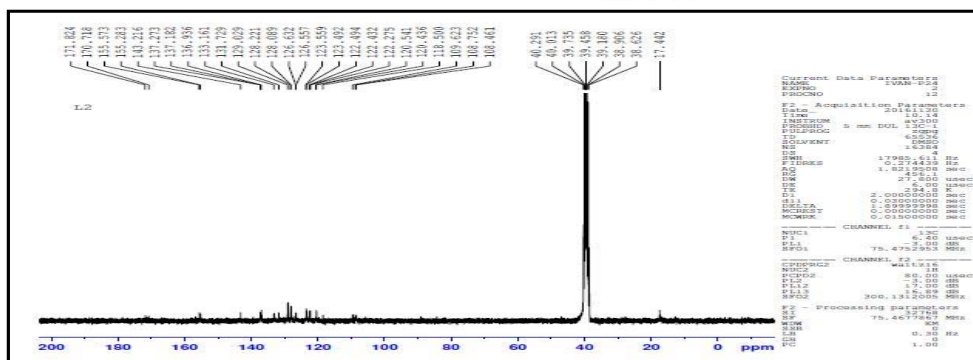
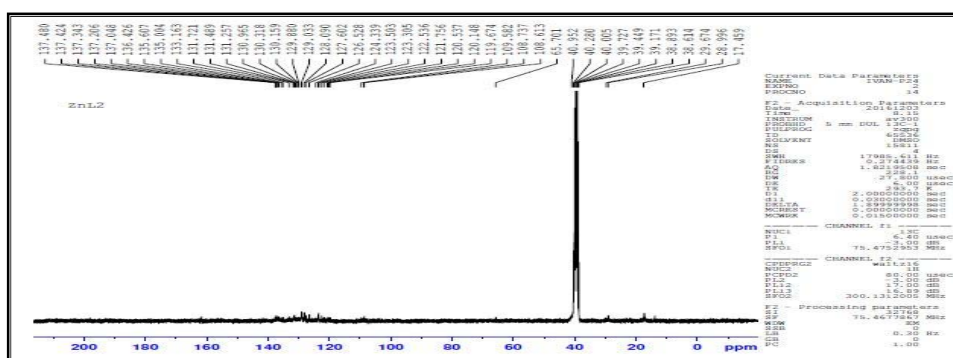


Figure (12): ¹H-NMR spectrum of [ZnL²] complex

Figure (13): ^{13}C -NMR spectrum of the ligand $[\text{H}_2\text{L}^2]$ 

Inhibition zone diameter (mm)

Figure (14): ^{13}C -NMR spectrum of $[\text{ZnL}^2]$ complex

Bacterial activity

The antibacterial activity for synthesized ligands and their metal complexes were studied against four bacterial species (*Escherichia coli*, *Enterobacter cloacae*, *Staphylococcus aureus* and *Bacillus*). The aim was understanding their potential antimicrobial activity. Separated studies were carried out with the solutions of DMSO (alone) to check the role of DMSO in the biological screening; these studies showed no activity against the bacterial strains tested [28]. Tables (12) give the measured zones of inhibition against the growth of different bacteria, the effect of the synthesized compounds on bacterial strains displayed in Fig. (15). The antimicrobial activity depends on two factors; difference in the ribosomes of microbial cells and the impermeability of the microbial cells. Data information obtained (shown in the tables), reveals two important points:

1- Compared to the free ligands, it was found that the complexes were potentially more active against the bacterial strains tested, which may mean that the complexation increases antimicrobial activity. This may be due to (chelation effect) in which the partially sharing of the metal positive charge in complexes by the donor atoms of the ligand. Also the π -electron delocalisation over the whole chelate ring increases the lipophilic character of the metal chelate system. This will result in increasing of its permeation through lipid layer of the cell membranes of the microorganism [28 & 29].

2- Zinc (Zn^{II}) complexes may have the higher antimicrobial activity compared with the other complexes. This may be due the electronic configuration (d^{10} system) and their higher molecular weight, compared with other metal complexes.

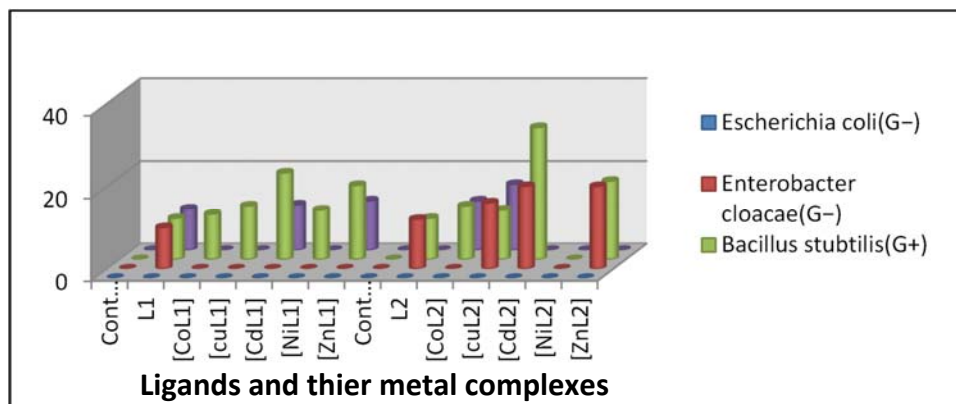


Figure (15): Evolution of diameter zone (mm) of inhibition of $[H_2L^1]$, $[H_2L^2]$ and their complexes against the growth of various bacterial strains.

Conclusions

According to the elemental analysis, conductance and magnetic studies [which shown in table (11)] along with the mentioned spectral data a tetrahedral geometry were proposed for the complexes. Some of the prepared compounds have antibacterial activity against the tested bacteria.

References

- [1] B. Priya and S.Lakhmi, Int. J. Chem. Tech. Res. 6(1), 87-94. 2014.
- [2] M. Aslam; I. Anis; N. Afza; Z. Noreen and L. Iqbal, Mol. Clin. Pharm., 4, 26-31, 2013.
- [3] Section 11.6: Imine (schiff base) formation- Chem., Wiki.
- [4] Sh .Jadhava; M. Raia; F. B. Ansarib and R. K. Pardeshic, J. Chem., Pharm., 8(1):245-249, 2016 .
- [5] F. A. Bassyouni; H. A. Tawfik; A. Soliman; M. Abdel Rehim and Res Chem Intermed, 38, 1291-310, 2012.
- [6] M. R. H. Keypour, 280, 203-53, 2014.
- [7] S.R. Salman and Nai'l A.I. Saleh, Can. J. Anal. Sci. Spectrosc 42(1), 9. 1997.
- [8] A. M. Asiri and K. O. Badahdah. Mol, 12, 1796-1804, 2007.
- [9] O. Thomas; O. Ingnas and R.M., Andersson., Macromolecules 31, 2676-2678. 1998.
- [10] A.R.R.D, A.Tzchoppe; J.Korbmacher; A.K.Azad; C.H.Cuppens and C.Korbmacher, the Journal of physiology, ew588, 1211, 2010.
- [11] C.J. Pouchert, "The Alderich Library of Infrared Spectra" 3rd, Edition, 1950.
- [12] R. M. Silverstein, "Spectrometric Identification of Organic Compounds "7th edition, John Willey and Son, inc., 174, 2005.
- [13] Y.R.Sharma "Organic Spectroscopy Principles and Chemical Application" Iso. 9001, 2000.
- [14] F. Karipcin and E. Kabalcilar, Acta. Chim. Slov, 54, 242-247, 2007.
- [15] W. M. Alwan, "M.Sc. Thesis", University of Baghdad college of Education (Ibn-Al-Haitham), 2006.

- [16] F.R.Ali, "M.SC. Thesis", University of Baghdad college of Education (Ibn-Al-Haitham), 2014.
- [17] E. Erdem; E.Y.Sari; R. Kinlincarslan and N. Kabay, *Trans.Met.Chem.,Dol*, 008-9173, 2008.
- [18] D.Sakthilatha; R.RaJavel and J. Chem, *Pharm. Res* , **5** (1):57-63,2013.
- [19] M. Usharani; E. Akila, and R. Rajavel , *Inter. J .* , **5** (3), 2013.
- [20] X. D. West; W. Kaminsky; I. K. Goldber; P. J. Jasinski and R.Woudenberg, *J. Mol.Struct*, **608**, 135-141,2002.
- [21] H. Colchoubian; WL. Waltz and J.W. Quail, *Can. J.Chem.*, 37-77, 1999.
- [22] J.W. Ledbetter and J. *Phys. Chem*70-2245. , 1966.
- [23] A.B.P. Lever, "*Inorganic Electronic Spectroscopy*", second ed, Elsevier Publishing,NewYork, 1984.
- [24] S. Chandra; M. Pundir, *Spectrochim. Acta, Part* , 69, 2008.